Volume 14 Number 18 1986 Nucleic Acids Research

Alkyl phosphotriester modified oligodeoxyribonucleotides. VI. NMR and UV spectroscopic studies of ethyl phosphotriester (Et) modified R_p-R_p and S_p-S_p duplexes, {d[GGAA(Et)TTCC]}$_2$

Michael F.Summers*, Cindy Powell[1], William Egan, R.Andrew Byrd, W.David Wilson[1] and Gerald Zon[2]*

Biophysics Laboratory and [2]Molecular Pharmacology Laboratory, Division of Biochemistry and Biophysics, Food and Drug Administration, 8800 Rockville Pike, Bethesda, MD 20892 and [1]Department of Chemistry and Laboratory for Microbial and Biochemical Sciences, Georgia State University, Atlanta, GA 30303-3053, USA

Received 26 June 1986; Revised and Accepted 28 August 1986

ABSTRACT

^{1}H NMR chemical shift assignments for the title compounds were made for all but a few H_5' and H_5'' signals using two-dimensional nuclear Overhauser effect (2D-NOE) data, which was also used for the first time to assign absolute configuration at phosphorus. The chemical shifts were, in general, similar to those reported [Broido, M.S., et al. (1985) Eur. J. Biochem. 150, 117-128] for the B-like conformation of the unmodified, parent duplex, [d(GGAATTCC)]$_2$. Differences in chemical shifts for corresponding protons were mostly localized to the AA(Et)TT region, and showed some stereochemical dependence. Unambiguous assignment of the phosphotriester ^{31}P signals was achieved in a novel way using selective insensitive nucleus enhancement by polarization transfer (selective INEPT) NMR. The R_p-R_p duplex melted ca. 11 °C lower than either the S_p-S_p or parent duplexes, as evidenced by T_m and variable temperature ^{1}H/^{31}P NMR measurements. The 2D-NOE data for the R_p-R_p duplex suggested possible steric interactions between the ethyl group and the H_3' of the flanking A residue. At low ionic strength, the S_p-S_p and parent duplexes had similar stability but at high ionic strength the S_p-S_p duplex was less stable.

INTRODUCTION

Synthetic oligonucleotides that have backbone modifications are useful as model compounds for studying DNA structure and dynamics,[1-4] and as probes for elucidating specific interactions of DNA with proteins and enzymes.[5-11] Such investigations, which must address the issue of chirality at phosphorus, have dealt mostly with molecules that have phosphorothioate linkages, the absolute configurations of which can be readily assigned by enzymatic procedures.[2,6,7] Stereochemical studies of methanephosphonate analogues of oligonucleotides have used X-ray crystallographic[4,12] and NOE measurements[13] to determine chirality at phosphorus in dimers, while methyl and ethyl phosphotriester internuleotide linkages, which are relevant to recognition and repair processes,[14] have been heretofore stereochemically defined by CD and NMR methods, but again only at the dimer-level.[15-19] Recent syntheses of isopropyl[20] and ethyl[11,21,22] phosphotriester modified oligonucleotides by the phosphoramidite method has led to the development[11,20-22] of a general,

chemo-enzymatic scheme for assigning the absolute configuration at phosphorus in such triesters, as discussed in detail in the accompanying paper.[22] Although there is compelling evidence to support the correctness of this configurational correlation scheme, the final assignments are nevertheless dependent on assumptions regarding the stereochemical course of the chemical and enzymatic reactions which are utilized. It was desirable to have an independent spectroscopic method that would both firmly establish the chirality of alkyl phosphotriester linkages and, moreover, provide details about the conformation and dynamics of the backbone modified oligonucleotides. 2D-NOE and other NMR methods that have been successfully applied[23-26] to synthetic oligonucleotides were therefore investigated, and we now wish to report ^1H-^1H 2D-NOE and variable temperature NMR/UV studies of the prototypal, diastereomeric, ethyl phosphotriester-modified octanucleotide duplexes, $\underline{R}_p$-$\underline{R}_p$ and $\underline{S}_p$-$\underline{S}_p$ {d[GGAA(Et)TTCC]}$_2$. The results clearly establish absolute configuration at phosphorus and thus confirm the assignments based on chemical and enzymatic reactions.[22] The presently reported spectroscopic investigations have also provided new insights to the structural and dynamical effects of backbone ethylation on double stranded DNA. The significance of these results and the general applicability of the spectroscopic methods are discussed.

EXPERIMENTAL

The $\underline{R}_p$ and $\underline{S}_p$ diastereomers of d[GGAA(Et)TTCC] were co-synthesized, separated by HPLC, obtained as their sodium salts, and stereochemically identified by procedures described elsewhere.[22]

NMR Measurements

NMR measurements were made with a JEOL GX-400 NMR spectrometer (399.65 MHz, ^1H; 161.7 MHz, ^{31}P) equipped with a variable temperature controller which maintained the sample to ±0.1 °C. Samples were prepared in D_2O (99.8 atom-% D) containing either potassium phosphate (PO_4, 0.01 M), or piperazine-$\underline{N}$,$\underline{N}$'-bis-(2-ethanesulfonic acid) (PIPES, 0.01 M) buffer at pH 7.0; the "pH" values (pH*) for D_2O-containing solutions correspond to observed readings with a pH-meter and were not corrected for possible isotope effects. Other sample conditions are given in the legends to the figures. The chemical shifts were referenced to internal H_2O or HOD.

^1H NMR spectra of the exchangeable protons were obtained using the 1-3-3-1 pulse sequence; relevant parameters have been published.[25]

Absorption mode 2D-NOE data[27] were obtained using the JEOL GX-400

spectrometer to control the experiment and detect the ^1H signals, which were digitized, signal averaged, and processed with a Nicolet 1280 computer. The spectrometer conditions were as follows: 4-kHz spectral width; 2048 data points in t_2; 250 μs per t_1 value; 128 data points collected in t_1, zero-filled to 512 points; 250-ms mixing time; 3-s repetition delay.

Selective $^{31}P\{^1H\}$ INEPT[28] experiments were performed in a manner similar to previously reported $^{13}C\{^1H\}$[29-31] and $^{15}N\{^1H\}$[32] methods using the following conditions: 4-kHz spectral width; 4096 data points; $\Delta_1/2 = \Delta_2/2 = 30$ msec, 25-msec selective 90° ^1H pulse; 6-Hz Gaussian broadening prior to Fourier transformations. The chemical shifts were referenced to external trimethylphosphate-H_2O (1% v/v).

UV Spectral and T_m Measurements

Oligomer UV spectral analysis and melting experiments were performed on a Cary 219 spectrophotometer interfaced to an Apple IIe microcomputer through a bidirectional digital communication port. Up to 5 cells were monitored and thermostatted in a 5-position rotatable cell turret. The temperature control was through a Haake PG20 temperature programmer connected to a Haake A81 refrigerated water bath. Temperature was monitored by a Cary 219 thermistor unit with the thermistor sealed in the reference cuvette which contained the appropriate buffer and was in position 1 of the turret. Other cuvettes had Teflon stoppers and all were 1-cm pathlength reduced-volume quartz cells. Nitrogen gas was passed continuously through the sample compartment of the Cary 219 during low temperature measurements. Digitized absorbance values were plotted as a function of temperature on the Cary 219 chart recorder and were simultaneously stored by the computer for subsequent plotting and analysis. The computer collected 10 absorbance readings and averaged them for each point on the T_m curve to improve signal-to-noise. T_m measurements were initiated either at 0 °C or slightly below 0 °C, and the temperature ramp was 0.5 °C/min. For the relatively broad T_m curves obtained for the DNA oligomers, adsorbance readings were collected only once per min, and this typically resulted in more than 50 points for a transition curve. PIPES buffers used throughout these experiments contained 10 mM PIPES, 1 mM EDTA, and NaCl as follows: PIPES 00, no added NaCl; PIPES 10, 0.1 M NaCl; PIPES 20, 0.2 M NaCl; PIPES 40, 0.4 M NaCl; PIPES 100, 1.0 M NaCl. All of these buffers were adjusted to pH 7.0.

RESULTS AND DISCUSSION

^1H-^1H 2D-NOE and Absolute Configuration at Phosphorus

A contour plot of the 2D-NOE data for the $\underline{R_p}$-$\underline{R_p}$ duplex is given in Fig.

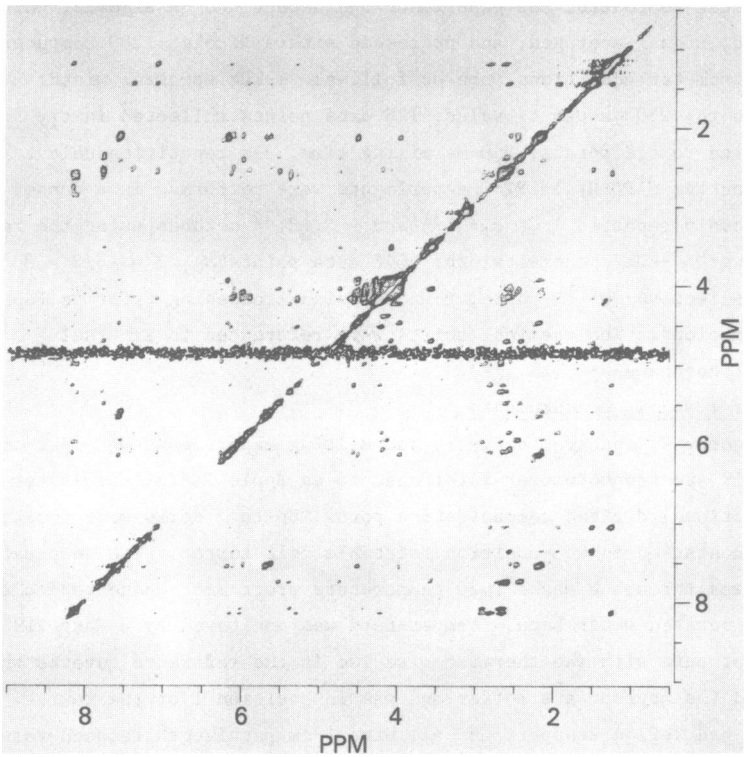

Fig. 1. Absorption-mode 2D-NOE spectrum of the ($\underline{R}_p$-$\underline{R}_p$) duplex; 0.3 mM in PO_4-D_2O pH* 7, 5 °C.

1. Except for cross-peaks involving the ethyl group (vide infra) and the noise at 4.90 ppm resulting from incomplete HDO saturation, the spectrum was similar to that published for the non-ethylated, parent compound.[23] The 2D-NOE data were analyzed in the usual manner[23,33-35] which led to assignment of all but a few of the H_5' and H_5" signals, as given in Table I. For comparison, chemical shift assignments previously determined[23] for the parent compound are also given in Table I. The similarity of the cross-peak patterns observed for the $\underline{R}_p$-$\underline{R}_p$ and $\underline{S}_p$-$\underline{S}_p$ (spectra not shown) duplexes relative to the parent duplex suggested that the ethyl groups in each case did not grossly alter the B-type conformation found[23] for the parent structure. On the other hand, a few of the cross-peak intensities are substantially different. Specifically, both the $\underline{R}_p$-$\underline{R}_p$ and $\underline{S}_p$-$\underline{S}_p$ duplexes display weaker-than-normal NOE cross-peaks between T5-H_6 and T5-H_2', H_2" protons and between T5-H_1' and

Table I. ^{1}H NMR Chemical Shift Assignments for R- and S-[d(GGAA(P(O)(OEt))TTCC)]$_2$ and for [d(GGAATTCC)]2[a]

Residue[b]		H_8	H_6	H_5	CH_3	H_1'	H_2'	H_2''	H_3'	H_4'	H_5'	H_5''
G1	P	7.80				5.62	2.47	2.68	4.80	4.19	3.66	3.66
	S	7.75				5.50	2.42	2.60	4.72	4.06	3.54	3.54
	R	7.72				5.50	2.42	2.60	4.73	4.05	3.50	3.50
G2	P	7.80				5.42	2.65	2.74	5.00	4.33	4.13	4.05
	S	7.75				5.36	2.61	2.67	HDO	4.25	-	4.06
	R	7.72				5.35	2.60	2.65	5.01	4.30	4.13	4.08
A3	P	8.16				6.04	2.74	2.96	5.09	4.48	(4.22	4.16)
	S	8.10				5.99	2.66	2.90	5.01	4.40	4.17	4.11
	R	8.05				5.97	2.65	2.87	5.00	4.41	4.18	4.14
A4	P	8.16				6.20	2.61	2.96	5.03	4.50	4.33	4.28
	S	8.15				6.13	2.64	2.80	5.27	4.53	4.18	4.20
	R	8.11				6.01	2.65	2.72	5.22	4.51	4.17	4.17
T5	P		7.20		1.29	5.93	2.02	2.58	4.48	4.37	4.22	4.14
	S		7.06		1.23	5.87	1.93	2.57	4.73	4.19	-	-
	R		6.95		1.27	5.77	1.85	2.52	4.58	4.25	-	4.03
T6	P		7.40		1.58	6.12	2.19	2.58	4.91	4.22	4.22	4.13
	S		7.37		1.49	6.10	2.12	2.56	HDO	4.15	-	-
	R		7.41		1.50	6.10	2.12	2.55	HDO	4.18	-	-
C7	P		7.54	5.68		6.02	2.16	2.47	4.84	4.37	(4.22	4.14)
	S		7.53	5.60	-	5.96	2.12	2.46	HDO	4.10	-	-
	R		7.55	5.6		5.84	2.15	2.43	HDO	4.10	-	-
C8	P		7.50	5.51		6.18	2.28	2.28	4.56	4.19	4.05	4.01
	S		7.56	5.70	-	6.15	2.14	2.19	4.49	3.95	4.09	-
	R		7.58	5.7		6.14	2.16	2.19	4.45	3.91	4.05	3.99

[a] Data for the non-alkylated parent oligonucleotide were taken from ref. 23; T = 20 °C, 0.18M NaCl; 0.1M PO_4 buffer; 0.2M EDTA; pH* = 7.0. Sample conditions for the data obtained in this study are as follows: T = 5° C; no added NaCl; 0.01 M PO_4 buffer; pH* = 7.0; [R_p-R_p] = [S_p-S_p] = *ca.* 0.3 mM; reference = internal HDO (4.84 ppm). [b] The letters P, R, and S refer to the parent compound, and the R_p, and S_p ethylated octamers, respectively (ref. 22). The numbering of the base residues is in the 5'→3' direction: $d(G_1G_2A_3A_4T_5T_6C_7C_8)$.

T5-H_2', H_2'' protons. The nature of these differences in intensity is unclear at this time, but may be attributed, at least in part, to increased flexibility and motion.[33] Conformational changes might account for these differences in cross-peak intensity; indeed, comparison of chemical shift results (*vide infra*) indicated that there were localized structural differences between the R_p-R_p and S_p-S_p duplexes. In contrast, cross-peaks between A4-H_1' and T5-CH_3, T5-H_1' and T6-CH_3, A4-H_3' and T5-CH_3, T5-H_3' and T6-CH_3, C7-H_5 and T6-CH_3, and C7-H_5 and C7-H_2', H_2'' were stronger than those expected for normal B-DNA. However, the 2D-NOE spectrum published by Broido *et al.*[23] displays anomalous intensities among these same cross-peaks and, consequently, the origin of these effects is unrelated to the presence of the

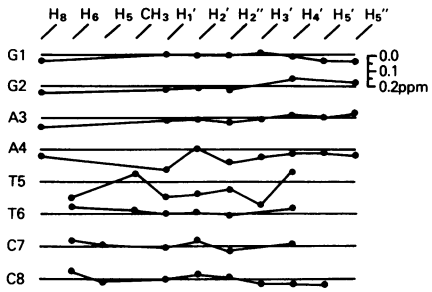

Fig. 2. Diagram of chemical shift differences for $\underline{R}_p$-$\underline{R}_p$ and $\underline{S}_p$-$\underline{S}_p$ duplexes listed in Table I.

ethyl groups. A detailed quantitative study of the time-dependent NOE's to establish the reasons for these intriguing intensity patterns was beyond the scope of the presently reported investigations, although such work is currently being initiated.

Small but significant chemical shift differences (>0.05 ppm) between corresponding proton signals were found for the ethylated duplexes, and, moreover, these chemical shift differences were confined primarily to signals for the dA and dT residues which flank the ethyl phosphotriester moiety, as shown graphically in Fig. 2. While it remains to be established whether or not these spectral features result from subtle differences in geometry and conformation about the phosphotriester group, as described for adenosine 5'-$\underline{O}$-(diethyl phosphate),[36] it is interesting that similar effects on proton chemical shifts for base residues adjacent to a modified phosphate linkage have been observed (James, T.L. and Zon, G., unpublished work) for diastereomeric duplexes of the phosphorothioate-containing analogue, d($GG_sAATTCC$).

Slices from the 2D-NOE data which display cross-peaks associated with the ethyl group of the $\underline{R}_p$-$\underline{R}_p$ duplex are shown in Fig. 3; no similar cross-peaks between the ethyl group and the rest of the molecule were observed for the $\underline{S}_p$-$\underline{S}_p$ duplex. In the $\underline{R}_p$-$\underline{R}_p$ duplex, the ethyl-CH_2 gives a cross-peak with A4-H_3' (Fig. 3c), while the A4-H_3' proton displays cross-peaks with both the ethyl-CH_2 and ethyl-CH_3 protons (Fig. 3b). Inspection of framework and space-filling models of ethyl phosphotriester internucleotide linkages in B-form DNA clearly indicates that in the $\underline{R}_p$ configuration (Fig. 4) there are shorter internuclear distances (hence stronger NOE's) between the ethyl group protons and the flanking H_3', as compared to those for the $\underline{S}_p$ configuration.

These findings were consistent with the chemo-enzymatically assigned absolute stereochemistry at phosphorus.[22] The relative distances and NOE's hold for other diastereomeric, backbone-modified, B-form oligonucleotides, in

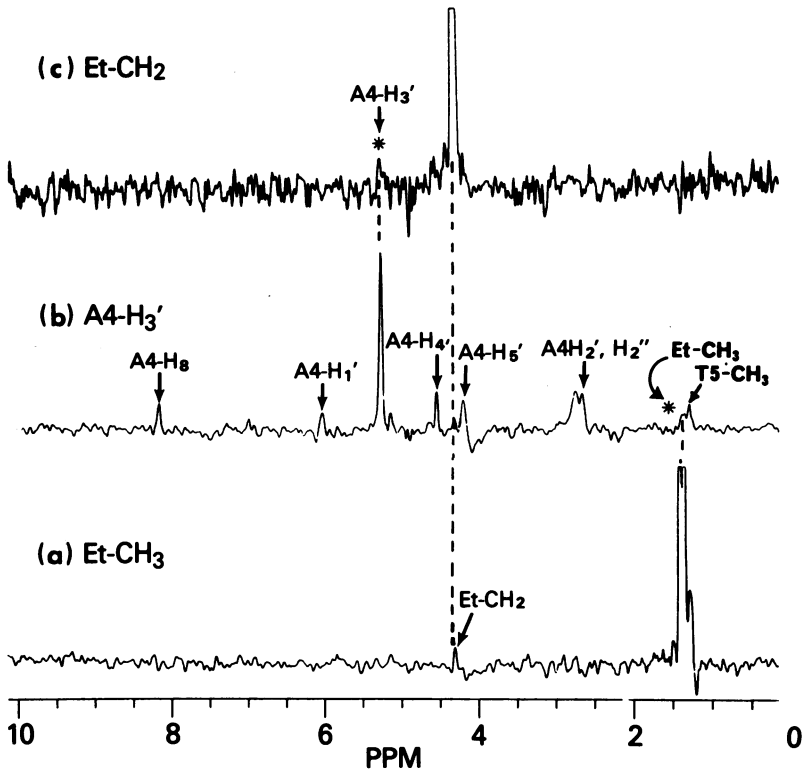

Fig. 3. Slices corresponding to the indicated diagonal peaks from the contour plot in Fig. 1 showing cross-relaxation between protons of the ethyl group and A4-H_3' (b,c). In (a), only one weak cross peak was observed due to the long relaxation time of the Et-CH_3 and relatively short pulse delay employed.

a sequence-independent manner, which implies that the method described here can have general applicability. Evidence which supports this conclusion has been obtained in 2D-NOE studies (Summers, M.F. and Zon, G., unpublished work) of the diastereomerically pure, isopropylated duplexes,[20] $\{d[GGAA(iPr)TTCC]\}_2$ and $\{d[CGCG(iPr)CG]\}_2$, wherein the NMR-assigned $\underline{S}_p$ (NOE) and $\underline{R}_p$ (no NOE) configurations were confirmed by enzymatic excision of d[N(iPr)N'] for chemical correlation with $d(N_SN')$. [Note that d(...N(Et)N'...) and d(...N(iPr)N'...) having the same relative configuration at phosphorus will have different absolute stereochemical designations due to changes in group priority.] Methanephosphonate (P-CH_3) modified oligonucleotides, $\{d[GGAA(P\text{-}CH_3)TTCC]\}_2$, as separate $\underline{R}_p$-$\underline{R}_p$ (no NOE) and $\underline{S}_p$-$\underline{S}_p$ (NOE) duplexes, $\{d[GGAA(P\text{-}CH_3)TTCC]\}_2$, have likewise given (Summers, M.F. and Zon, G.,

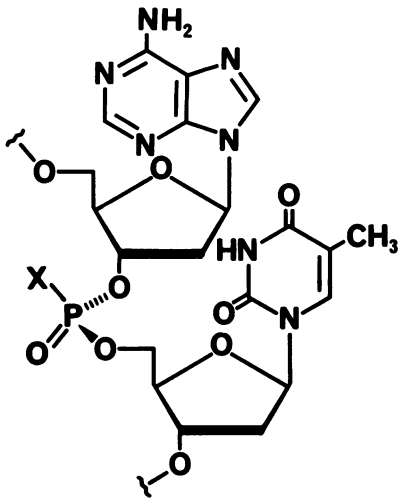

R_p X=OEt
S_p X=OiPr
S_p X=Me

Fig. 4. Orientation of substituent X toward the major groove in B-DNA.

unpublished work) stereochemically characteristic 2D-NOE spectra that were correlated with the X-ray crystallographically-derived absolute configuration at phosphorus in the enzymatically excised dimer, d[A(P-CH_3)T].[12,37] In each of the aforementioned cases where cross-peaks were observed between a pendant alkyl substituent and the DNA chain, cross-relaxation included H_3' of the 5'-flanking deoxyribosyl residue, and, in some cases, H_6 of the 3'-flanking pyrimidine residue.

Selective INEPT Phosphorus Spectra

^{31}P NMR spectra of the ethylated $\underline{R}_p$-$\underline{R}_p$ and $\underline{S}_p$-$\underline{S}_p$ duplexes are shown in Fig. 5. In each case, 7 distinguishable ^{31}P NMR signals were observed at low temperature (5 °C), consistent with a single time-averaged structure for each duplex, wherein the 14 phosphate groups comprise 2 identical (by rotation) sets of 7 heterotopic (chemically nonequivalent) internucleotide linkages. In each case, 6 signals have chemical shifts (ca. -3.8 to -4.7 ppm) similar to those which have been found[38a] for the parent octamer, while the remaining signal was located ca. 1.6 ppm upfield. The chemical shift of the upfield signal was consistent with that expected for an ethyl phosphotriester; however, it is well-known that structurally altered oligonucleotides can exhibit anomalous chemical shifts. Several possible techniques for

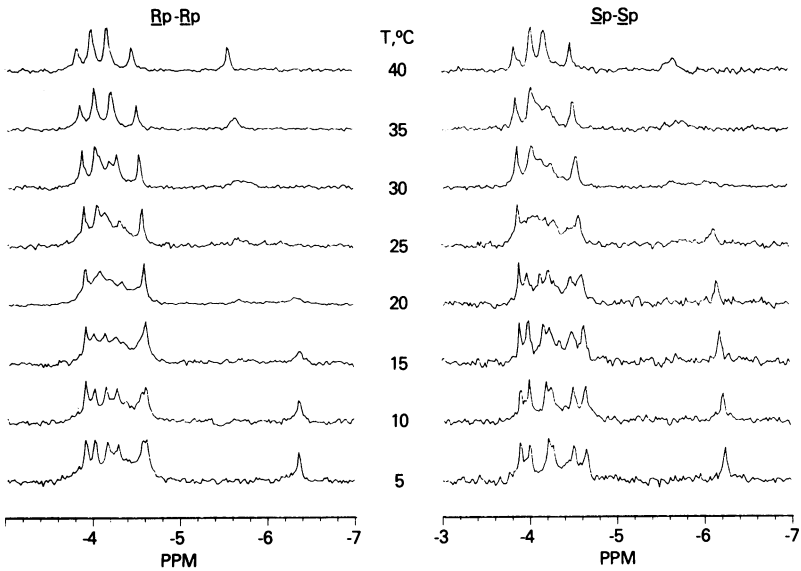

Fig. 5. Variable temperature ^{31}P NMR spectra of $\underline{R}_p$ and $\underline{S}_p$ ethylated octamers.

unambiguously identifying the phosphotriester signals were considered. ^{17}O-labeling of DNA could be used[7,26,38] as well as a double-resonance technique ($^1H\{^{31}P\}$),[39a] although newer 2D ^1H-^{31}P chemical shift correlation spectroscopy is more efficient.[26,39b] Our alternative approach utilized selective INEPT NMR, which was recently developed and reported[28,31,32] as a general one-dimensional method for assignment of a heteronucleus via polarization transfer through scalar coupling with a proton whose chemical shift has been assigned. The unambiguous assignment of any given phosphodiester resonance signal may thus be obtained by this method provided that a flanking H_3', H_4' or H_5', $5''$ proton resonance is well-resolved. This study is the first application of selective INEPT for assignment of ^{31}P signals. Fig. 6A shows the ^{31}P NMR spectrum of the $\underline{R}_p$-$\underline{R}_p$ ethylated duplex at 5 °C in PO_4-buffered solution (the signal at ca. -1.9) ppm is due to internal PO_4). Using selective irradiation of the A4-H_3' proton signal, a selective INEPT spectrum was obtained (Fig. 6B) which clearly identified the high-field ^{31}P signal as A4-P-T5.

Variable Temperature Phosphorus and Proton NMR: Stereochemical Effects

The upfield ^{31}P NMR signal for the phosphotriester group in each of the ethylated octamers was monitored over a temperature range of 5 to 40 °C (Fig. 5) as a means of studying the local melting behavior of these

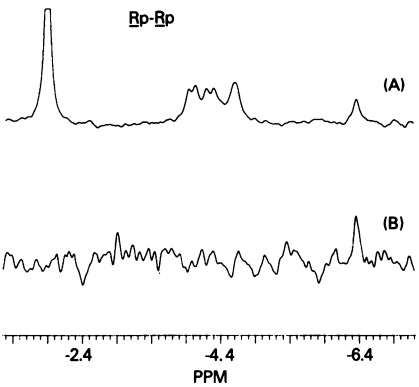

Fig. 6. ^{31}P NMR (A) and selective INEPT (B) spectra of $\underline{R}_p$-$\underline{R}_p$ duplex.

compounds, at the site of modification, for comparison with T_m measurements by UV spectroscopy. The ^{31}P NMR spectra for the $\underline{R}_p$-$\underline{R}_p$ and $\underline{S}_p$-$\underline{S}_p$ duplexes at 5 °C both showed a pair of signals at -3.90 and -4.05 ppm. Signals with essentially the same chemical shifts had also been exhibited by the parent duplex and were assigned[38a] by ^{17}O-labeling to the 3'- and 5'-terminal dinucleoside phosphates, d(CpC) and d(GpG), respectively. In view of the 3-nucleotide spacing between these terminal residues and the phosphotriester group in the ethylated duplexes, the -3.90 and -4.05 ppm signals seen in Fig. 5 at 5 °C were tentatively assigned to the d(CpC) and d(GpG) terminal linkages, respectively. While other individual phosphodiester signals were not assigned, the virtual superposability of their downfield-shifted (ca. 0.2 ppm) high-termperature pattern was consistent with single-stranded, random coil oligonucleotides, and showed that these resonances were not detectably influenced by the stereochemistry of the phosphotriester linkage. The reason(s) for the more pronounced downfield shift (ca. 0.6-0.7 ppm) of the ethyl phosphotriester signals upon melting are not clear at the present time. In any event, this large chemical shift difference led to marked exchange-broadening of the ethyl phosphotriester signals upon melting, with the observation of separate signals for double- and single-stranded molecules (cf. Fig. 5, 20-30 °C). These results suggested that the $\underline{R}_p$-$\underline{R}_p$ duplex had a melting point ca. 10 °C less than that of the $\underline{S}_p$-$\underline{S}_p$ duplex under the conditions employed. The parent duplex lacked appropriately distinguishable ^{31}P signals, and a melting measurement by ^{31}P NMR was not possible.

As an independent means of studying the melting of {d[GGAA(Et)TTCC]}$_2$ for comparison with the parent compound, the ^1H NMR spectra (not shown) of the Watson-Crick imino (NH-N) protons were monitored over a temperature range of

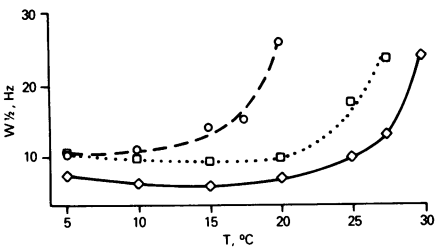

Fig. 7. Half-height width vs. temperature for A4-T5 NH-N signal of parent (◇), $\underline{S}_p$ (□), and $\underline{R}_p$ (○) octamers in 10 mM PIPES pH*7 at 0.6 mM.

5 to 40 °C. In each case, the terminal G-C proton signal was the first to broaden and disappear with increasing temperature. Measurement of half-height widths of the central A4-T5 signals as a function of temperature was of interest since these NH-N protons are nearest to the site of modification. From plots (Fig. 7) of these data it was deduced that (1.) duplex stability apparently decreased in the order: parent ~ $\underline{S}_p$-$\underline{S}_p$ > $\underline{R}_p$-$\underline{R}_p$; and (2.) the apparent melting point of the $\underline{R}_p$-$\underline{R}_p$ duplex was ca. 10 °C below that of the parent and $\underline{S}_p$-$\underline{S}_p$ duplexes. These findings were consistent with the ^{31}P results. Interestingly, the more destabilized duplex, namely $\underline{R}_p$-$\underline{R}_p$, had also shown NOE cross-relaxation between protons on the alkyl group and the DNA. The same relation for duplex destabilization and the observation of NOE's between protons of the alkyl group and the flanking nucleotides was also found (Summers, M.F. and Zon, G., unpublished work) for the diastereomers of $\{d[CGCG(iPr)CG]\}_2$ and the diastereomers of $\{d[GGAA(P\text{-}CH_3)TTCC]\}_2$, which suggested that the destabilization may be predominantly a consequence of steric interactions between the alkyl group and the flanking nucleotides.

For comparative purposes, it is worthwhile to note here that ^1H NMR and NOE measurements for d(GGATCC) and its $\underline{N}^6$-methyl analogue, d(GGm^6ATCC), have shown that both oligonucleotides exist as B-DNA at low temperature, and that the apparent T_m values determined by exchange broadening were 45 and 32 °C, respectively.[40] This 13 °C decrease in T_m caused by $\underline{N}^6$-methylation of the two dA residues in $[d(GGm^6ATCC)]_2$ is similar in magnitude to the ca. 10 °C decrease in thermal stability reported here for the bis-ethylated $\underline{R}_p$-$\underline{R}_p$ duplex. In contrast to these effects, the set of four duplexes with the general structure $[d(CGNGAATTCm^6GCG]_2$, N=A,G,C, or T exhibit T_m values 19-26 °C lower than the T_m of the parent dodecamer.[41] It would thus appear that the destabilization of a duplex caused by $\underline{O}^6$-methylation of a dG residue is considerably greater than that caused by either $\underline{N}^6$-methylation of dA residues or $\underline{O}$-ethylation of internucleotide phosphate groups.

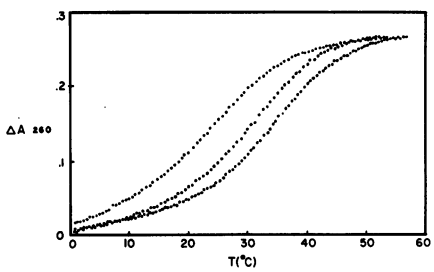

Fig. 8. Melting curves for $\underline{R}_p$, $\underline{S}_p$, and parent octamers (left to right), 0.15 mM bases in PIPES 20.

UV Spectral and T_m Measurements

Absorbances of solutions of the $\underline{R}_p$ and $\underline{S}_p$ diastereomers of the ethylated octamer in PIPES 20 buffer at 5 °C were normalized to the same absorbance at 258 nm, which is the absorbance maximum for both oligomers, and the samples were scanned from 320 to 250 nm. The resultant spectra were identical within experimental error, indicating similar base stacking in both diastereomers in the duplex state.

Melting studies, on the other hand, illustrated a pronounced difference in the stabilities of the $\underline{R}_p$-$\underline{R}_p$ and $\underline{S}_p$-$\underline{S}_p$ duplexes. Representative melting curves for these duplexes and the parent duplex in PIPES 20 buffer are shown in Fig. 8. Broad melting curves are observed since the helix to single-strand transitions have relatively low cooperativity in short oligomers. The curves were monophasic and thus indicated that no significant amount of a hairpin[25] conformation was formed under these conditions as the temperature was increased. Each curve was asymmetric on the low temperature side which suggested that terminal base pair unstacking occurred before duplex dissociation. In the PIPES 20 buffer (Fig. 8) the $\underline{S}_p$-$\underline{S}_p$ diastereomer melted *ca.* 4 °C lower than the parent duplex, while the $\underline{R}_p$-$\underline{R}_p$ diastereomer melted *ca.* 11 °C lower than the parent duplex.

Melting curves like those shown in Fig. 8 were obtained for the oligomers over a range of salt concentrations. Monophasic transitions were obtained at all salt concentrations, and the T_m values for the unsubstituted and ethylated duplexes isomers were plotted as a function of ionic strength (Fig. 9). The T_m values in 1 M salt do not increase as much as with other similar increases in salt concentration, and results obtained at that ionic strength were not included in drawing the lines in Fig. 9. The slopes for both the $\underline{R}_p$-$\underline{R}_p$ and $\underline{S}_p$-$\underline{S}_p$ diastereomers have values of 10.1 ± 0.1, which were not different within experimental error. The value of 14.6 for the slope of the unsubstituted parent oligomer was larger, as expected based on the greater charge density of this oligomer. The slopes of the plots which include the 1

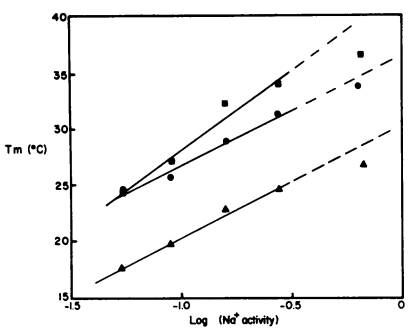

Fig. 9. UV-derived T_m vs. log (Na^+ activity) for $\underline{R}_p$ (▲), $\underline{S}_p$ (●), and parent (■) octamers.

M salt-points are 11.7, 9.2, and 8.5 for the parent, $\underline{S}_p$-$\underline{S}_p$, and $\underline{R}_p$-$\underline{R}_p$ duplexes, respectively.

The most striking feature of Fig. 9 is the significant difference in T_m values for the $\underline{R}_p$-$\underline{R}_p$ and $\underline{S}_p$-$\underline{S}_p$ diastereomers at all salt concentrations. These results provide strong evidence that the destabilization of the $\underline{R}_p$-$\underline{R}_p$ duplex is not simply the result of an electrostatic effect, and indirectly support the hypothesis (vide supra) that destabilization results predominantly from steric interactions. From the T_m difference between the $\underline{R}_p$ and $\underline{S}_p$ cases in Fig. 9, the difference in thermal stability between these diastereomers is ca. 11 °C over the entire salt range. The unsubstituted oligomer behaves in a manner similar to the $\underline{S}_p$ case. As can also be seen in Fig. 9, the parent and $\underline{S}_p$ oligomers have similar stability at low salt concentration. At higher ionic strengths, where electrostatic effects are less important, the unsubstituted oligomer is more stable. Direct steric effects do not appear able to account for the destabilization of the $\underline{S}_p$-$\underline{S}_p$ duplex relative to the parent nucleotide, and it will thus be of interest to evaluate relative stabilities for other sequences to determine whether this is a common feature of neutral versus charged phosphate linkages.

CONCLUSIONS

In general, the ^1H NMR chemical shifts for protons of the $\underline{R}_p$-$\underline{R}_p$ and $\underline{S}_p$-$\underline{S}_p$ duplexes of d[GGAA(Et)TTCC] were very similar to those reported by Broido et al.[23] for the parent (non-alkylated) oligonucleotide. Shift differences greater than 0.05 ppm were primarily localized to the central A(Et)T region of the molecule, which presumably reflects minor structural differences, while protons in other regions of the oligonucleotides gave nearly identical ^1H NMR chemical shifts, which presumably indicates structural congruency.

The T_m measurements and variable temperature $^1H/^{31}P$ NMR spectra obtained with the diastereomeric duplexes, {d[GGAA(Et)TTCC]}$_2$, provided a self-consistent set of data which indicated that the melting characteristics of these backbone-modified helices were markedly dependent upon the absolute stereochemistry of the ethyl phosphotriester linkage. The near-equivalence of the T_m values for the $\underline{S}_p$-$\underline{S}_p$ and parent duplexes, despite the lower charge density in the former compound, suggested that simple electrostatic considerations regarding duplex stability may be misleading. Thus, the ca. 7-11 °C lower melting temperature found at all salt concentrations for the $\underline{R}_p$-$\underline{R}_p$ duplex, relative to the $\underline{S}_p$-$\underline{S}_p$ and unmodified duplexes, together with the stereochemically dependent NOE's indicate that unfavorable steric interactions may be operative, although more data for different sequences and different substituents will be needed to clarify these points. Further studies of this sort may also resolve apparent anomalies in the thermal stabilities noted recently for complexes of poly (U)·d[A(R)A], R = Me, Et, 2,2,2-trichloroethyl, wherein the role of steric effects has been questioned.[42]

The NOE-derived assignments of absolute configuration at phosphorus in the $\underline{R}_p$-$\underline{R}_p$ and $\underline{S}_p$-$\underline{S}_p$ diastereomers of {d[GGAA(Et)TTCC]}$_2$ agree with the assignments made using a chemo-enzymatic approach.[22] From this work and other ongoing studies that have been referred to, it appears that for phosphate-alkylated oligonucleotides the stereoisomer with the alkyl group oriented "toward the major groove" gives characteristic NOE cross-peaks between the alkyl group and H_3' of the 5'-flanking nucleotide and, in some cases, H_6 (or H_8) of the 3'-flanking nucleotide. In addition, the stereoisomer with the alkyl group oriented "into the solvent" (away from the major groove) lacks these NOE's, and exhibits melting behavior similar (if not identical) to that of the parent oligonucleotide. In contrast, the inward-oriented alkyl group leads to significantly lower melting temperatures. The UV-derived T_m vs. salt concentration profiles support the hypothesis that this duplex destabilization is primarily a consequence of steric effects. Complete 2D-NOE/energy-minimization structural analyses and thermodynamic studies of these ethylated oligonucleotides have been initiaed in our laboratories to further elucidate the consequences of alkylating DNA phosphate groups.

ACKNOWLEDGMENT

A portion of this work was supported by NIH Grant GM 30267 to W.D.W.

*To whom correspondence should be addressed

REFERENCES

1. Miller, P.S., Dreon, N., Pulford, S.M. and McParland, K.B. (1980) J. Biol. Chem. 255, 9659-9665.
2. Cosstick, R. and Eckstein, F. (1985) Biochemistry 24, 3630-3638.
3. Suggs, J.W. and Taylor, D.A. (1985) Nucleic Acids Res. 13, 5707-5716.
4. Callahan, L., Han, F.-S., Watt, W., Duchamp, D., Kezdy, F.J. and Agarwal, K. (1986) Proc. Natl. Acad. Sci. USA 83, 1617-1621.
5. Miller, P.S., Chandrasegaran, S., Dow, D.L., Pulford, S.M. and Kan, L.S. (1982) Biochemistry 21, 5468-5474.
6. Connolly, B.A., Eckstein, F. and Pingoud, A. (1984) J. Biol. Chem. 259, 10760-10763.
7. Stec, W.J., Zon, G., Egan, W. and Stec, B. (1984) J. Am. Chem. Soc. 106, 6077-6079.
8. Noble, S.A., Fisher, E.F. and Caruthers, M.H. (1984) Nucleic Acids Res. 12, 3387-3404.
9. Eppstein, D.A., Schryver, B.B. and Marsh, Y.V. (1986) J. Biol. Chem. 261, 5999-6003.
10. Stollar, B.D., Zon, G. and Pastor, R.W. (1986) Proc. Natl. Acad. Sci. USA 83, 4469-4473.
11. Koziolkiewicz, M., Uznanski, B., Stec, W.J. and Zon, G. (1986) Chem. Scr. 26, 251-260.
12. Chacko, K.K., Lindner, K., Saenger, W. and Miller, P.S. (1983) Nucleic Acids Res. 11, 2801-2814.
13. Kan, L.S., Cheng, D.M., Miller, P.S., Yano, J. and Ts'o, P.O.P. (1980) Biochemistry 19, 2122-2132.
14. Modrich, P. (1982) CRC Crit. Rev. Biochem. 13, 287-323; Margison, G.P., Cooper, D.P. and Brennand, J. (1985) Nucleic Acids Res. 13, 1939-1952.
15. Potter, B.V.L., Eckstein, F. and Uznanski, B. (1983) Nucleic Acids Res. 11, 7087-7103.
16. Herdering, W. and Seela, F. (1985) J. Org. Chem. 50, 5314-5323.
17. Weinfeld, M., Drake, A.F., Saunders, J.K. and Paterson, M.C. (1985) Nucleic Acids Res. 13, 7067-7077.
18. Hamblin, M.R. and Potter, B.V.L. FEBS Lett. (1985) 189, 315-317.
19. Drake, A.F., Kuroda, R., Livingston, D.C. and Weinfeld, M., private communication.
20. Stec, W.J., Zon, G., Gallo, K.A., Byrd, R.A., Uznanski, B. and Guga, P. (1985) Tetrahedron Lett. 26, 2191-2194.
21. Uznanski, B., Koziolkiewicz, M., Stec, W.J., Zon, G., Shinozuka, K. and Marzilli, L.G. (1986) Chem. Scr. 26, 221-224.
22. Gallo, K.A., Shao, K.-I., Phillips, L.P., Regan, J.B., Koziolkiewicz, M., Uznanski, B., Stec, W.J. and Zon, G., accompanying paper.
23. Broido, M.S., James, T.L., Zon, G. and Keepers, J. (1985) Eur. J. Biochem. 150, 117-128.
24. Jamin, N., James, T.L. and Zon, G. (1985) Eur. J. Biochem. 152, 157-166.
25. Summers, M.F., Byrd, R.A., Gallo, K.A., Samson, C.J., Zon, G. and Egan, W. (1985) Nucleic Acids Res. 13, 6375-6386.
26. Byrd, R.A., Summers, M.F., Zon, G., Fouts, C.S. and Marzilli, L.G. (1986) J. Am. Chem. Soc. 108, 504-505.
27. States, D.J., Haberkorn, R.A. and Ruben, D.J. (1982) J. Magn. Reson. 48, 286-292.
28. Byrd, R.A., unpublished work.
29. Sorensen, O.W. and Ernst, R.R. (1983) J. Magn. Reson. 55, 338-343.
30. Bax, A. (1984) J. Magn. Reson. 57, 314-318.
31. Bax, A., Egan, W. and Kovac, P. (1984) J. Carbohydr. Chem. 3, 593-611.
32. Bax, A., Niu, C.-H. and Live, D. (1984) J. Am. Chem. Soc. 106, 1150-1151.
33. Feigon, J., Denny, W.A., Leupin, W. and Kearns, D.R. (1983) Biochemistry 22, 5930-5942.

34. Scheek, R.M., Boelens, R., Russo, N., van Boom, J.H. and Kaptein, R. (1984) Biochemistry 23, 1371-1376.
35. Wemmer, D.E., Chou, S.-H., Hare, D.R. and Reid, B.R. (1984) Biochemistry 23, 2262-2268.
36. Brennan, R.G., Kondon, N.S. and Sundaralingam, M. (1984) J. Am. Chem. Soc. 106, 5671-5676.
37. Stec, W.J., Zon, G., Egan, W., Byrd, R.A., Phillips, L.R. and Gallo, K.A. (1985) J. Org. Chem. 50, 3908-3913.
38. (a.) Connolly, B.A. and Eckstein, F. (1984) Biochemistry 23, 5523-5527; (b.) Joseph, A.P. and Bolton, P.H. (1984) J. Am. Chem. Soc. 106, 437-439; (c.) Petersheim, M., Mehdi, S. and Gerlt, J.A. (1984) J. Am. Chem. Soc. 106, 439-440.
39. (a.) Cheng, D.M., Kan, L.-S., Iuorno, V.L. and Ts'o, P.O.P. (1984) Biopolymers 23, 575-592; (b.) Pardi, A., Walker, R., Rapoport, H., Wider, G. and Wuthrich, K. (1983) J. Am. Chem. Soc. 105, 1652-1653; (c.)Lai, K., Shah, D.O., DeRose, E. and Gorenstein, D.G. (1984) Biochem. Biophys. Res. Commun. 121, 1021-1026; (d.) Marion, D. and Lancelot, G. (1984) Biochem. Biophys. Res. Commun. 124, 774-783.
40. Fazakerly, G.V., Teoule, R., Guy, A., Fritzsche, H. and Guschlbauer, W. (1985) Biochemistry 24, 4540-4548.
41. (a.) Gaffney, B.L., Marky, L.A. and Jones, R.A. (1984) Biochemistry 23, 5686-5691; (b.) Patel, D.J., Shapiro, L., Kozlowski, S.A., Gaffney, B.L., Jones, R.A. (1986) Biochemistry 25, 1027-1036.
42. Letsinger, R.L., Bach, S.A. and Eadie, J.S. (1986) Nucleic Acids Res. 14, 3487-3499.